

Scientific Paper

Doi: <http://dx.doi.org/10.1590/1809-4430-Eng.Agric.v44e20230088/2024>

## DESIGN OF KEY COMPONENTS FOR A NEW RAPESEED WINDROWER

Junhui Ran<sup>1,2\*</sup>, Can Hu<sup>1,2</sup>, Wensong Guo<sup>1,2</sup>, Xufeng Wang<sup>1,2</sup>

\*Corresponding author. College of Mechanical and Electronic Engineering, Tarim University/Alar, China. Modern Agricultural Engineering Key Laboratory at Universities of Education Department of Xinjiang Uygur Autonomous Region, Tarim University/Alar, China. E-mail: 120200005@taru.edu.cn | ORCID ID: <https://orcid.org/0009-0002-5032-1163>

### KEYWORDS

rapeseed, windrower, cutting mechanism, reel, planetary gear mechanism.

### ABSTRACT

Rapeseed cutting and sunning are important processes associated with rapeseed harvesting in China. However, existing rapeseed windrowers have problems such as a tendency to entangle rapeseed plants, low laying quality, low operational efficiency, and high cutting power consumption for tall rapeseed plants. Hence, a new type of rapeseed windrower was designed. A new cutter with a planetary gear driving double moving cutting bars was designed, a motion model of the planetary gear mechanism was established, and the motion and structural parameters of the cutter were analysed. A theoretical analysis of this new cutting system showed that it not only had low cutting impact, minimal disturbance to rapeseed stalks, and high cutting continuity, but also low power consumption and stable operating performance. A reel based on a double-crank planar five-link mechanism was designed, and kinematics modelling and analysis of the new reel were carried out. The structure and motion parameters for the new reel were obtained. Finally, field experiments were conducted on both the newly designed rapeseed windrower and the original one. The results indicated that the newly designed windrower was suitable for high-quality, efficient cutting and sunning operations for tall rapeseed plants.

### INTRODUCTION

Rapeseed is a major oil crop in China, and its plants and pods have unique structural and physical characteristics. Most varieties of Chinese rapeseed plants are tall, and have thick stems with numerous branches that intersect with each other; the seeds are small, and mature pods are prone to cracking. In addition, the connection strength between rapeseed pods and branches is low (Wu, et al., 2017), and they easily fall off under external forces such as the impact of a reel and disturbance from a cutter. These characteristics of rapeseed have given rise to difficulties in mechanised harvesting, resulting in high loss rates, high power consumption and low efficiency (Wu et al., 2018; Zhan et al., 2022). When rapeseed is harvested in combination, due to its complete maturity, the loss rate is high (usually over 8%); rapeseed pods that are not harvested in a timely manner naturally crack, resulting in a greater loss rate. Harvesting methods such as picking and threshing after cutting and

sunning can not only reduce these harvest losses, but also exploit the post-ripening effect of rapeseed to reduce its moisture content and improve its quality. In addition, this approach can avoid risks to the harvest arising from extreme weather conditions such as strong winds and hail (Guan et al., 2021). Hence, the procedure of cutting and sunning has become an accepted process of rapeseed harvesting in China.

However, due to the high overall moisture content of rapeseed plants (usually higher than 75%), they have great resilience during the windrower operation. This not only causes high power consumption during cutting and sunning operations, but also makes it easy for the cut rapeseed plants to become entangled in the reel, which affects the quality and efficiency of the operation (Qing et al., 2021). The laying quality of rapeseed in the field after it is cut not only directly affects the effectiveness of crop drying and post ripening, but also significantly affects the losses caused by subsequent processes such as rapeseed picking and threshing. As one of the core components of the windrower, the functions of the

<sup>1</sup> College of Mechanical and Electrical Engineering, Tarim University/Alar, China.

<sup>2</sup> Modern Agricultural Engineering Key Laboratory at Universities of Education Department of Xinjiang Uygur Autonomous Region, Tarim University/Alar, China.

Area Editor: João Paulo Arantes Rodrigues da Cunha

Received in: 6-16-2023

Accepted in: 1-24-2024

reel are to guide and support the crop to be cut by the cutter, and to push the final cut crop towards the rear of the header to prevent the crop from accumulating in front of the header (Ran et al., 2020). The performance of the reel therefore has a significant impact on the operation of the rapeseed windrower. At present, the rapeseed windrowers used in China mainly use ordinary rotary or eccentric reels (Liang et al., 2018), and rapeseed can easily become wrapped around these when cutting tall plants. This reduces the quality of harvesting and increases the loss rate. In addition, the single-action knife cutter driven by a crank connecting rod or sway ring on a rapeseed harvester (Ma et al., 2020; Chai et al., 2018; Li et al., 2021) not only has high levels of vibration and power consumption, but also causes great disturbance to the rapeseed stems, which can easily increase the rapeseed harvest loss rate (Ren et al., 2018).

Hence, improving the quality and efficiency of the reel operation and reducing the disturbance to rapeseed plants caused by the cutter are of great significance in order to improve the quality and efficiency of rapeseed planting. The reciprocating double-action cutter not only has characteristics such as good running balance performance, low vibration, and low stubble cutting, but also has low power consumption for cutting and high efficiency, making it suitable for cutting tall, thick stems (Guan et al., 2019; Shen et al., 2016). A reciprocating double-action cutter is therefore used in harvesters for tall, thick crops such as ramie. However, the existing reciprocating double-action cutter uses a crank linkage mechanism to drive the cutter bars. Due to the large inertia force generated during the movement of the crank linkage mechanism, the reciprocating cutter bars typically generate a lateral force on the tool holder, which can result in high-frequency impact of the moving cutter bar on the tool holder, high levels of vibration, and even breakage of the cutter bar (Yang et al., 2019). In addition, in order to reduce the loss of rapeseed caused by the impact of the reel on rapeseed plants, the installation position of the reel on the rapeseed harvester has been adjusted, the harvesting loss has been reduced by extending the header (Wang et al., 2017),

and scholars have also explored ways to reduce the rapeseed harvest loss rate by increasing the rotation radius of the reel and reducing the tine bar speed of the reel. However, the effectiveness of the current windrower when applied to tall, thick rapeseed plants is still poor, and the quality and efficiency of this operation still need to be improved.

In view of these problems with the rapeseed windrower, in this study, based on the structure and physical characteristics of the tall, thick rapeseed plants in China, a windrower with a new cutter and reel was designed to ensure high-quality and efficient cutting and sunning operations for rapeseed plants. Firstly, a double action cutter with low stem disturbance, low vibration and power consumption and high efficiency was developed, and a mechanism driven by a planetary gear was designed to give a compact double-action cutter with smooth transmission. Then, based on a kinematics analysis of the double-crank five-link mechanism, a reel was designed to ensure good results when applied to tall, thick rapeseed plants with high moisture content. Finally, the actual performance of the designed rapeseed windrower was verified through field experiments.

### Structure and principle of operation of the proposed rapeseed windrower

The overall structure of the rapeseed windrower is shown in Fig. 1. As the core part of the windrower, the header first separates the intersecting branches of the rapeseed plants inside and outside of the cutting pair, through the use of vertical cutters on both sides, thereby avoiding pulling between uncut and already cut rapeseed during operation, which reduces the loss rate. The tine bars on the reel then transfer the rapeseed to be cut to the horizontal cutter, and provide support to allow the cutter to cut the rapeseed. Following this, the cut rapeseed plants are pushed further towards the header by the tine bars. Finally, the conveyor belt on the header transports the rapeseed plants to the field directly below the machine, thereby completing the laying of the rapeseed.

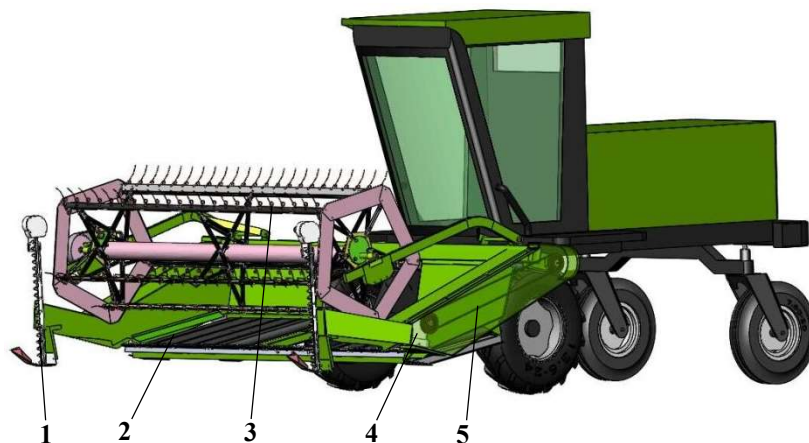


FIGURE 1. Overall structure of the windrower: (1) vertical cutter; (2) conveyor belt; (3) new reel; (4) planetary gear-driven mechanism of the horizontal double action cutter; (5) belt.

**Structure and principle of operation of the horizontal double action cutter and its driving mechanism**

**Structure and principle of operation of the planetary-gear-driven mechanism of the horizontal double action cutter**

The double action cutter planetary gear driver is shown in Fig. 2, and mainly consists of a pulley, a small bevel gear, a large bevel gear, a planetary gear component, a rack, and a fixed shaft gear. Power is input into the driver by the pulley, and the planetary carrier is driven to rotate through a pair of bevel gears. The planetary gear component installed on the

planetary carrier then meshes with the gear ring on the box (Fig. 2a), and the crankshaft on the planetary gear component moves in a reciprocating straight line through the centre of the gear ring. The active gear rack articulated on the crank shaft drives a cutter bar to move while meshing with the fixed shaft gear (Fig. 2b), thus driving the passive gear rack that is also meshed with the fixed shaft gear and connected to another cutter bar; this causes it to move in a reciprocating straight line direction that is opposite to the active gear rack, ultimately achieving reciprocating motion of the upper and lower cutting knives.

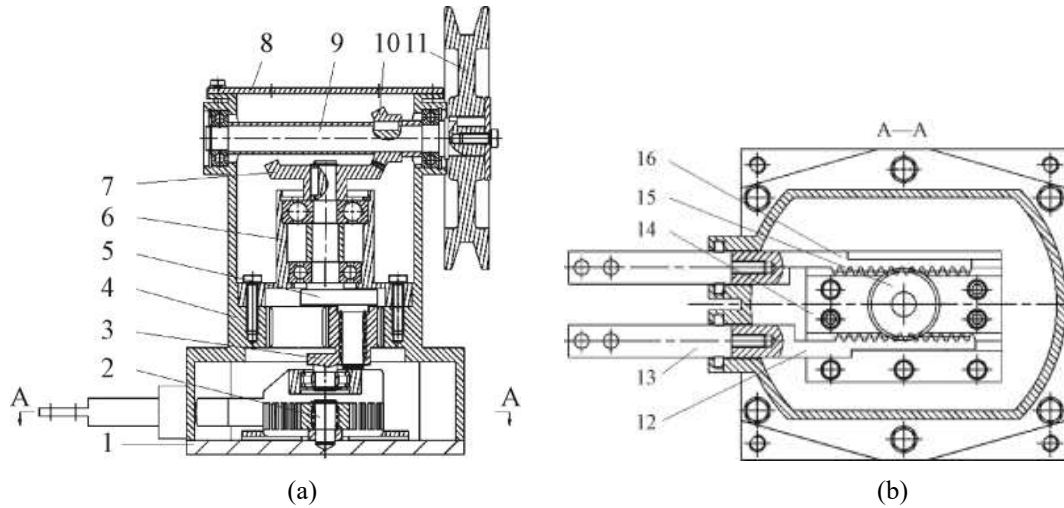


FIGURE 2. Structural diagram of the planetary gear driver for the double action cutter. (a) Front view: (1) bottom cover; (2) axle of fixed-shaft gear; (3) planet gear assembly; (4) box; (5) planet carrier; (6) support of planet carrier; (7) large bevel gear; (8) top cover; (9) axle of belt wheel; (10) small bevel gear; (11) belt wheel. (b) Local sectional view: (12) passive rack; (13) connecting rod; (14) chute; (15) fixed-shaft gear; (16) active rack.

**Overall structure and principle of operation of the cutter**

The overall structure of the cutter is shown in Fig. 3. During operation, the upper and lower moving knife bars always move in opposite directions at equal speeds, and the rapeseed stems are cut by the two blades cutting in both

directions simultaneously. Hence, its stability during operation is high, and its cutting ability is strong. In addition, compared to a traditional single-blade cutter, this design has a light weight and a simple structure, as the need for blade protectors and fixed blades is eliminated.

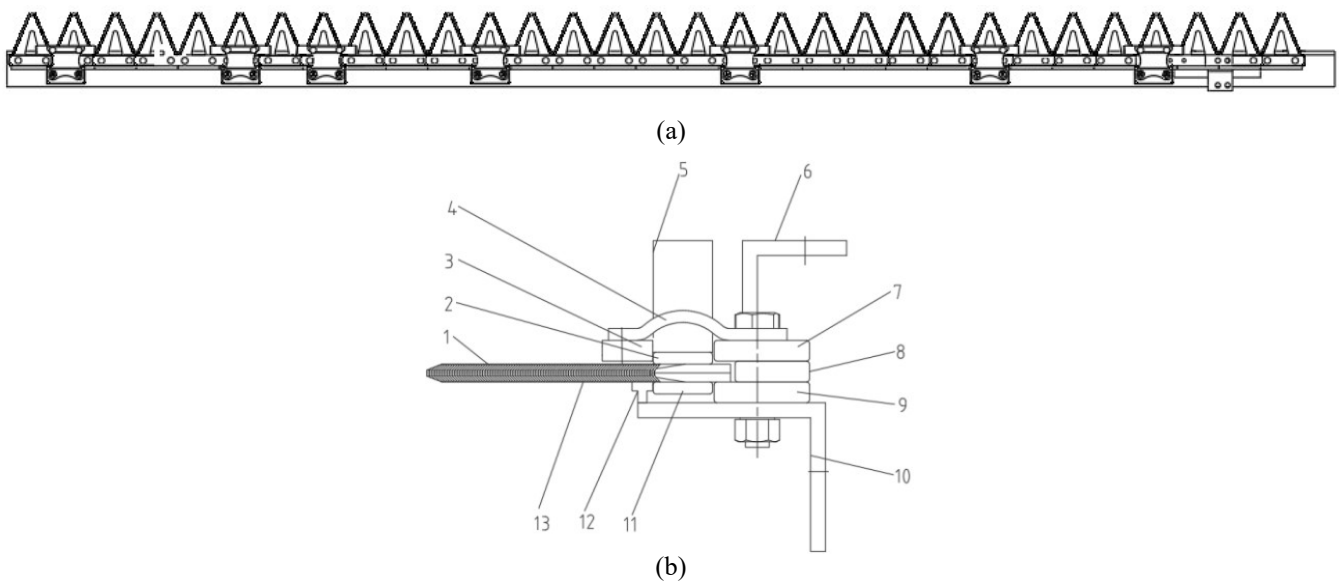


FIGURE 3. Diagram of the cutter. (a) Top view of the cutter. (b) Left view of the cutter: (1) upper moving blade; (2) upper moving blade rod; (3) front positioning block of the upper blade rod; (4) blade press; (5) upper moving blade connecting rod; (6) lower moving blade connecting rod; (7) rear positioning block of the upper blade rod; (8) positioning block; (9) knife rod support block; (10) knife holder; (11) lower moving blade rod; (12) lower blade rod support strip; (13) lower moving blade.

**Structure and principle of operation of the reel**

A new type of reel structure based on a planar five-link mechanism is shown in Fig. 4. The power to the reel drive shaft is input through a sprocket, and the reel drive shaft rotates to drive the planar five-link mechanism. The five

linkage mechanisms are evenly distributed around the reel, as shown in Fig. 4 (b), and each linkage mechanism drives a tine bar to move along a specific trajectory. Each five-link mechanism of the tine bar undergoes the same motion pattern at the same position.

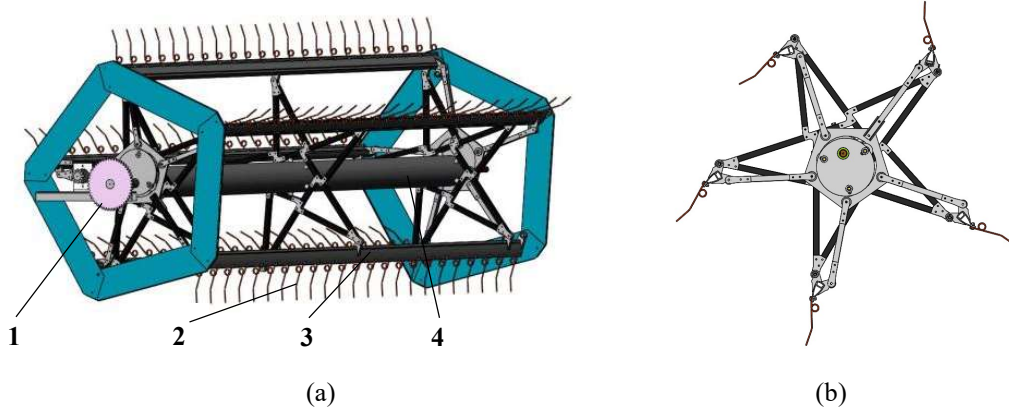


FIGURE 4. Proposed reel based on a planar five-link mechanism. (a) Structural diagram of the new reel: (1) sprocket; (2) tine bar; (3) support rod for the tine bar; (4) drive shaft of the reel. (b) Front view of the five-link structure of the reel.

The trajectories of the tine bar relative to the machine motion, the absolute motion, and the reel operation process are shown in Fig. 5. Firstly, from the contact between the reel and the rapeseed to the cutting of the rapeseed by the cutter under the support of the reel, the motion trajectory of the reel relative to the rapeseed is an absolute trajectory. During this process, the role of the reel is to move the rapeseed towards the cutter and provide support as the cutter cuts the rapeseed stems. When the rapeseed stem has been cut, the tine bars push the rapeseed onto the header and continue to push it backwards. In this process, the motion trajectory of the tine

bars relative to the rapeseed can be regarded as a relative motion trajectory. From Fig. 5, it can be seen that the relative motion trajectory of the tine bar is not a standard circular shape: when the tine bars have finished pushing the rapeseed and are about to leave, the radius of rotation of the tine bars suddenly decreases, and the curvature of the curve rapidly decreases. This allows the tine bars to quickly move away from the rapeseed, which helps to reduce the disturbance to the rapeseed caused by the tine bars and reduces the probability of the rapeseed wrapping around the tine bars.

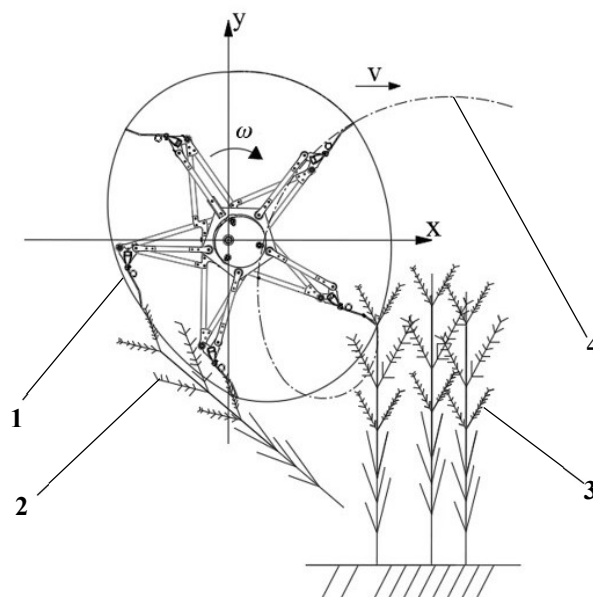


FIGURE 5. Schematic diagram showing the principle of operation of the new reel: (1) relative motion trajectory of the tine bar; (2) cut rapeseed plants; (3) rapeseed plants to be harvested; (4) absolute motion trajectory of the tine bar.

## MATERIAL AND METHODS

### Design of key parameters for the double-action cutting mechanism driven by planetary gears

#### Construction of a motion model for the double-action cutter planetary gear driver

The cutter driver of the planetary gear mechanism needs to convert rotary motion into the reciprocating linear motion of the cutter bar, meaning that the structural parameters of the planetary gear mechanism must meet certain conditions. The motion law of the planetary gear driver can be analysed based on the motion diagram shown in Fig. 6. The large and small circles in the diagram represent the indexing circles of the gear ring and planetary gear, respectively, and their radii are represented as  $R$  and  $r$ . The rotating arm  $OO_1$  rotates counterclockwise at an angular velocity of  $\omega$  to drive the planetary gear. At a certain moment, point A on the planetary gear indexing circle is located at the intersection point  $A_1$  of the X-axis and the gear ring, and after moving for time  $t$ , point A is located at the tangent point  $A_2$  of the planetary gear and the gear ring indexing circle, as shown in Fig. 6. At this point, the rotation angle of the rotating arm is  $\theta$ , the rotation angle of the planetary gear is  $\beta$ , and the angle between  $AO_1$  and the vertical direction is  $\alpha$ .

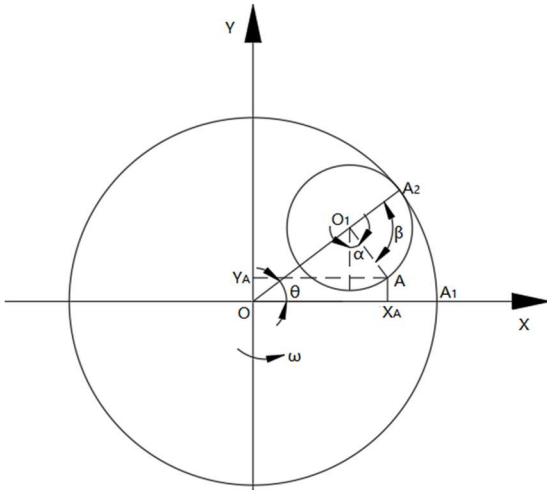


FIGURE 6. Schematic diagram showing the motion of the planet gear.

If the coordinates of point A are  $(X_A, Y_A)$ , then [eq. (1)] holds.

$$\begin{cases} X_A = OO_1 \cos \theta + r \sin \alpha \\ Y_A = -(r \cos \alpha - OO_1 \sin \theta) \end{cases} \quad (1)$$

If we consider the motion of the circle of the planetary gear as pure rolling, [eq. (2)] can be established.

$$\begin{cases} R\theta = r\beta \\ \theta = \omega t \end{cases} \quad (2)$$

As shown in Fig. 6,  $\alpha$  satisfies [eq. (3)].

$$\alpha = \frac{\pi}{2} - (\beta - \theta) \quad (3)$$

Combining [eq. (2)] and [eq. (3)] yields [eq. (4)]:

$$\alpha = \frac{\pi}{2} - \frac{R-r}{r} \theta \quad (4)$$

We then substitute [eq. (4)] into [eq. (1)] to obtain [eq. (5)]:

$$\begin{cases} X_A = OO_1 \cos \theta + r \cos\left(\frac{R-r}{r} \theta\right) \\ Y_A = -\left[r \sin\left(\frac{R-r}{r} \theta\right) - OO_1 \sin \theta\right] \end{cases} \quad (5)$$

From [eq. (5)], it can be seen that the motion trajectory of point A on any planetary gear indexing circle is an internal cycloid. To make it move only along the X-axis direction, both displacement and velocity in the Y-direction must be zero, that is, point A on the planetary gear indexing circle satisfies [eq. (6)].

$$\begin{cases} Y_A = -\left[r \sin\left(\frac{R-r}{r} \theta\right) - OO_1 \sin \theta\right] = 0 \\ \frac{dY_A}{dt} = -\left[(R-r) \cos\left(\frac{R-r}{r} \theta\right) - OO_1 \theta\right] = 0 \end{cases} \quad (6)$$

From Fig. 6, it can be seen that  $R$  satisfies [eq. (7)]:

$$R = r + OO_1 \quad (7)$$

By substituting [eq. (7)] into [eq. (6)], [eq. (8)] can be obtained as follows:

$$OO_1 = r = \frac{1}{2} R \quad (8)$$

By substituting [eq. (8)] into [eq. (1)], it can be seen that the displacement, velocity, and acceleration motion laws of point A along the X-axis direction satisfy [eq. (9)]:

$$\begin{cases} x_A = 2r \cos \theta = 2r \cos \omega t \\ v_A = \frac{dx_A}{dt} = -2r\omega \sin \omega t \\ a_A = \frac{dv_A}{dt} = -2r\omega^2 \cos \omega t \end{cases} \quad (9)$$

Where:

$x_A$ ,  $v_A$  and  $a_A$  represent the displacement, velocity and acceleration of point A, respectively.

From an analysis of the law of motion of the planetary gear, we see that when the length of the rotating arm of the planetary gear transmission mechanism is equal to half of the radius of the gear ring indexing circle and equal to the radius of the planetary gear indexing circle, the points on the planetary gear indexing circle move in a straight line and follow a simple harmonic motion. When the planetary gear transmission mechanism meets the above structural parameters, and if the cutter bar is connected to a certain point on the planetary gear indexing circle, the cutter can perform reciprocating linear motion according to the simple harmonic motion law shown in [eq. (9)].

According to [eq. (8)], in order to meet the motion conditions of the cutter bar, the number of teeth on the gear ring must be twice the number of teeth on the planetary gear, and the diameter of the gear ring indexing circle is equal to the stroke of the cutter bar. In order to reduce the frequency of reciprocating motion and the inertia force of the cutter bar, the theoretical stroke of a single moving blade is designed as 76.2 mm, equal to the spacing between the standard moving blades. The maximum distance between the two moving blades from the start to completion of cutting is 38.1 mm. If this distance is considered as the fixed blade distance  $t_0$ , then its relationship with the cutter stroke  $S$  and blade spacing  $t$  fulfils [eq. (10)]. Hence, the upper and lower blades of the double action cutter are equivalent to two "low-cutting type cutters" for simultaneous reverse cutting operations, which is very beneficial in terms of reducing the side bending caused by the blade's disturbance to the rapeseed stem, thereby reducing the loss of seeds at the header. In addition, compared to an actual low-cutting type cutter, these dual moving blades have no fixed blade, which makes the mechanism more adaptable to cutting and less prone to problems such as material blockage.

$$S = t = 2t_0 = 76.2\text{mm} \quad (10)$$

Based on the theoretical travel requirements of the cutter bar mentioned above and the design of the planetary gear parameters (reference), the module of the planetary gear is set to 2 mm, the number of teeth is set to 20, the module of the gear ring is 2 mm, and the number of teeth is 40. The actual cutter stroke is 80 mm, a value 3.8 mm larger than the blade spacing of 76.2 mm. In this case, the cutting speed is well utilised, and this design can effectively avoid the problems of incomplete cutting and knife jamming when cutting wet and lodging rapeseed stems.

#### Determination of the sliding cutting angle of the double-action cutter blade

The sliding cutting angle of the blade has an important impact on the performance and power consumption of the cutter. When selecting the sliding cutting angle, it is necessary to study the mechanical performance of the crop stem of the cutting object, to provide theoretical support for the selection of the sliding cutting angle of the blade (Sun et al., 2023). The condition for successful cutting of the stem is that the force acting on it from the moving blade must meet a certain equilibrium state. The force on the stem under cutting with a double-action cutter was analysed, and the force diagram is shown in Fig. 7.

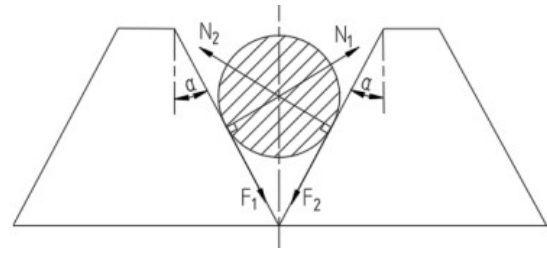


FIGURE 7. Forces on the stalk during double-blade cutting.

The condition under which the stem does not slide under the action of the blade is shown in [eq. (11)]:

$$(F_1 + F_2)\cos\alpha - (N_1 + N_2)\sin\alpha \geq 0 \quad (11)$$

Where:

$F_1$  and  $F_2$  are the frictional forces exerted by the two moving blades on the stem (N);

$N_1$  and  $N_2$  represent the support forces of the two moving blades on the stem (N);

$\alpha$  is the sliding cutting angle ( $^\circ$ ), and

$F_1$  and  $F_2$  satisfy the respective expressions in [eq. (12)]:

$$\begin{cases} F_1 = N_1 \tan\beta \\ F_2 = N_2 \tan\beta \end{cases} \quad (12)$$

Where:

$\beta$  is the friction angle of the stem ( $^\circ$ ).

As the same force is exerted by both moving blades on the stem,  $F_1$  and  $F_2$ ,  $N_1$  and  $N_2$  are of equal magnitude, and eqs. (11) and (12) can be solved together to obtain  $\tan\alpha \leq \tan\beta$ . Hence, the condition under which the stem does not slide when cut is shown in [eq. (13)]:

$$\alpha \leq \beta \quad (13)$$

The friction angle of the rapeseed stem is generally taken as  $\sim 20\text{--}25^\circ$ . However, since the blade used to measure the friction angle of crop stems is smooth, when selecting the sliding cutting angle for a toothed blade, a larger sliding cutting angle can be chosen to reduce the cutting resistance while ensuring cutting quality, due to the good clamping effect of the toothed blade on the stem. To ensure that the stem does not slide when cutting, the sliding angle of the blade was set to  $19^\circ$ . The blade inclination angle was  $20^\circ$ .

#### Theoretical analysis of the operating performance of the double-action cutter and its impact on the disturbance of rapeseed

The relationship between the motion speed and displacement of the newly designed cutting blade satisfies the elliptical expression in [eq. (14)], indicating that the velocity at a certain point on the edge of the blade changes relative to its displacement in accordance with the law governing an elliptical curve. From [eq. (14)], it can be seen that when  $x$  is zero (that is, a point on the cutting edge is at the midpoint of the cutter blade stroke), its speed reaches the maximum value

of  $2r\omega$ . When a certain point on the cutting edge is at the two extreme positions of the cutter stroke (i.e.  $x$  is  $-2r$  or  $2r$ ), the speed at that point will reach the minimum value, which is zero. When the double-action cutter operates, the upper and lower blades move at the same speed but in opposite directions, and each time the rapeseed stem is cut, the operation is completed in the middle of the cutter travel path. Hence, the cutting operation is completed at the highest speed of movement of the blade, which is conducive to the efficient cutting of rapeseed stalks. In addition, each blade of the cutter completes two cutting operations within one stroke; that is, as the planetary carrier of the planetary gear drive mechanism rotates once, the cutter achieves a total of four cutting operations. The proposed cutting mechanism therefore has high cutting efficiency and uniform load.

$$\frac{v_x^2}{4r^2\omega^2} + \frac{x^2}{4r^2} = 1 \quad (14)$$

The average speed of the cutter was calculated using [eq. (15)], and the ratio of this speed value to the forward speed of the machine was then used as the cutting speed ratio. Here, the value of the cutting speed ratio is 1.2.

$$v_p = \frac{2rn}{15} \times 10^{-3} \quad (15)$$

Since the double-action cutter cuts the stem through the simultaneous reverse movements of the upper and lower moving blade bars, it causes less disturbance to the rapeseed stem compared to a single moving blade. The maximum displacement of the double-action cutter blade with respect to the rapeseed stem is half of the distance between adjacent blades, which is 38.1 mm, as shown in Fig. 8a. However, the maximum displacement of rapeseed stalks by a single blade cutter can reach 76.2 mm, as shown in Fig. 8b. Hence, during the operation of the double-action cutter, the displacement of rapeseed stems is small, which reduces the brushing and collision between rapeseed plants, thereby helping to reduce the total loss rate of rapeseed harvest.

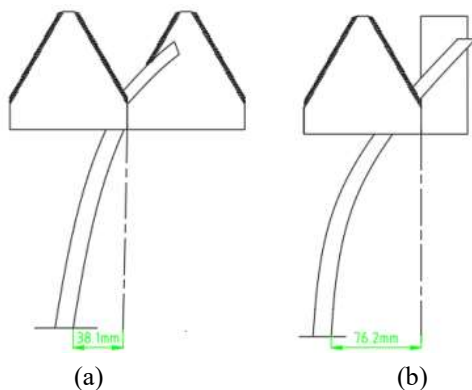


FIGURE 8. Maximum displacement of the rape stem under different cutting modes: (a) double-action cutter; (b) single-action cutter.

#### Analysis of the power consumption characteristics of the double-action cutter

The double-action cutter also has a positive effect in terms of reduced power consumption. The total cutting power consumption  $W$  consists of the idle power consumption  $W_k$  of

the cutting mechanism and the required power consumption  $W_g$  for cutting crops, as shown in [eq. (16)]. However, the idle power consumption of the cutter largely determines its total power consumption. If the driving mechanism is the same, the idle power consumption of the cutter is mainly determined by the kinetic energy of the cutter bar:

$$W = W_g + W_k = v_m B L_0 \times 10^{-3} + W_k \quad (kW) \quad (16)$$

Where:

$v_m$  is the forward speed of the machine ( $m \cdot s^{-1}$ );

$B$  is the machine cutting width (m), and

$L_0$  is the power dissipation required to cut per square meter area of stems ( $N \cdot m \cdot m^{-2}$ ).

Assuming that the kinetic energy of the single-action and double-action cutters are  $E_1$  and  $E_2$ , respectively, and the weight of each bar of the double-action cutter and the single moving blade bar are the same, then at the same cutting speed, [eq. (17)] holds. From [eq. (17)], it can be seen that the kinetic energy of a double-action cutter is half that of a single-action cutter, indicating that a double-action mechanism can significantly reduce idle power consumption.

$$\begin{cases} E_1 = \frac{1}{2} m v^2 \\ E_2 = \frac{1}{2} (2m) \left(\frac{1}{2} v\right)^2 = \frac{1}{4} m v^2 \end{cases} \quad (17)$$

Where:

$m$  is the total mass of a single bar component of the cutter (kg), and

$v$  is the speed of the single moving blade ( $m \cdot s^{-1}$ ).

#### Design of the five-link mechanism of the proposed reel

##### Motion model and structural parameter design of the five-link mechanism of the proposed reel

The horizontal plane was taken as the  $x$ -axis, the direction perpendicular to the horizontal plane as the  $y$ -axis, and point A as the coordinate origin to establish a Cartesian coordinate system. The planar five-link mechanism for the new type of reel was established as shown in Fig. 9.

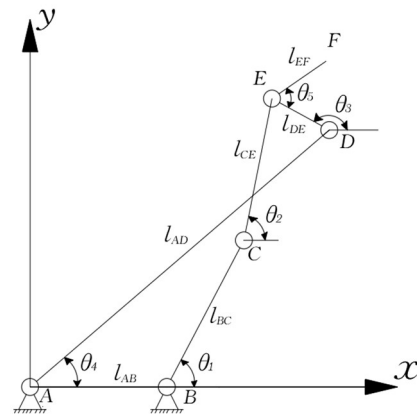


FIGURE 9. Schematic diagram of the five-link mechanism of the reel ( $l_{AB}$  is the rack;  $l_{BC}$  is the short crank;  $l_{AD}$  is the long crank;  $l_{DE}$  is a short connecting rod;  $l_{CE}$  is a long connecting rod;  $l_{EF}$  is the tine bar of the reel).

According to Fig. 9, the closed-loop vector equation for point E can be obtained as shown in [eq. (18)]:

$$\vec{l}_{AB} + \vec{l}_{BC} + \vec{l}_{CE} + = \vec{l}_{AD} + \vec{l}_{DE} \quad (18)$$

The above vector equation can then be decomposed along the x and y axes to obtain [eq. (19)]:

$$\begin{cases} l_{AB} + l_{BC} \cos \theta_1 + l_{CE} \cos \theta_2 = l_{AD} \cos \theta_4 + l_{DE} \cos \theta_3 \\ l_{BC} \sin \theta_1 + l_{CE} \sin \theta_2 = l_{AD} \sin \theta_4 + l_{DE} \sin \theta_3 \end{cases} \quad (19)$$

The motion equation of the tine bar of the wheel can be obtained from the laws of motion for rods AD and DE, or BC and CE. Since the steering for cranks AD and BC is the same and the angular velocity is equal, and both are known parameters, the values of  $\theta_4$  and  $\theta_1$  can be obtained at any time. In other words, as long as the angle between rods DE or CE and the x-axis ( $\theta_3$  or  $\theta_2$ ) is known at any time, the equation of motion of the tine bar can be obtained. In the five-link mechanism,  $\theta_3$  and  $\theta_2$  satisfy [eq. (20)], which can be solved by the Newton-Simpson iteration method:

$$\begin{cases} f_x(\theta_2, \theta_3) = l_{AB} + l_{BC} \cos \theta_1 + l_{CE} \cos \theta_2 - l_{DE} \cos \theta_3 - l_{AD} \cos \theta_4 \\ f_y(\theta_2, \theta_3) = l_{BC} \sin \theta_1 + l_{CE} \sin \theta_2 - l_{DE} \sin \theta_3 - l_{AD} \sin \theta_4 \end{cases} \quad (20)$$

The equation of motion for the tine bar is obtained from the laws of motion for rods BC and CE. At any time t, the motion trajectory equation of the tine bar relative to the machine in the x- and y-directions satisfies [eq. (21)].

$$\begin{cases} x_F = l_{AB} + l_{BC} \cos \theta_1 + l_{CE} \cos \theta_2 + l_{EF} \cos \theta_5 \cos \theta_3 \\ y_F = l_{BC} \sin \theta_1 + l_{CE} \sin \theta_2 + l_{EF} \cos(1.5\pi - \theta_5 - \theta_3) \end{cases} \quad (21)$$

Taking the ground as the reference frame and assuming the forward speed of the machine to be v, the motion trajectory of the tine bar relative to the ground in the x- and y-directions at any time t satisfies [eq. (22)]. By taking the first derivatives of eqs. (21) and (22), we can obtain the relative and absolute velocities of the tine bar, respectively. By calculating the second derivatives of eqs. (21) and (22), we obtain the accelerations of the relative and absolute motion of the tine bar, respectively.

$$\begin{cases} \dot{x}_F = \dot{l}_{AB} + \dot{l}_{BC} \cos \theta_1 + \dot{l}_{CE} \cos \theta_2 + \dot{l}_{EF} \cos \theta_5 \cos \theta_3 + vt \\ \dot{y}_F = \dot{l}_{BC} \sin \theta_1 + \dot{l}_{CE} \sin \theta_2 + \dot{l}_{EF} \cos(1.5\pi - \theta_5 - \theta_3) \end{cases} \quad (22)$$

In order to reduce the complexity of the mechanism and facilitate its transmission, the proposed planar five-link mechanism only has one free input crank, with the other crank turning the same direction and at the same angular velocity. Hence, the dimensions of the five-link mechanism need to meet the condition in [eq. (23)]:

$$l_{max} + l_{min1} + l_{min2} > m + n \quad (23)$$

Where:

$l_{max}$ ,  $l_{min1}$  and  $l_{min2}$  are the longest, shortest and second shortest lengths of the members of the mechanism, respectively, and

m and n represent the lengths of the other two members.

After the rapeseed plant has been cut, it is pushed onto the conveyor belt under the action of the reel, at a certain angle to the conveyor belt. At this time, if the tine bar cannot retract along the inclined direction of the rapeseed plant, it is likely to hang the fallen rapeseed plants. Hence, when the reel has completed the task of pushing the rapeseed plants, it is best for it to quickly move away from the plants to avoid entanglement with the reel or throwing it out of the header. In addition, the larger the radius of gyration of the tine bar, the larger the ring buckle it can form, which can effectively improve the ability of the harvesting wheel to push the plants and reduce the accumulation of cut plants on the header. The height of rapeseed plants in China is generally 800–1600 mm, with a stem diameter of 6–25 mm and a diameter of 400–600 mm in the pod layer. For the current rotary radius of the header of a windrower for tall, thick rapeseed plants, which is generally ~1000–1100 mm, the size range of the double-crank planar five-link mechanism reel is the same as that of an ordinary rapeseed windrower. We set  $l_{AB}$  as the frame,  $l_{BC}$  as the short crank,  $l_{AD}$  as the long crank, and the angle between the tine bar and the connecting rod  $l_{DE}$   $\theta_5$  to  $40^\circ$ . Based on the functional requirements of the double-crank planar five-link reel, and the known values of the parameters and other constraints, the parameters of the double-crank planar five-link mechanism were designed using Matlab software. Finally, the length parameters of each link in the double-crank planar five-link mechanism were obtained as  $l_{AB} = 54$  mm,  $l_{BC} = 157$  mm,  $l_{CE} = 358$  mm,  $l_{DE} = 80$  mm, and  $l_{AD} = 535$  mm. The initial angles between the short and long cranks and the horizontal plane were  $-30^\circ$  and  $-17^\circ$ , respectively.

#### Determination of the motion parameters of the new reel and its relative installation position on the header

According to the relevant technical requirements for the reel of a rapeseed windrower, the ratio of the tine bar speed of the new reel to the forward speed of the windrower is basically consistent with that of the original windrower. The relative motion trajectory of the tine bar in the five-link mechanism is irregular, and its speed is also constantly changing. In this study, we took the reel drive shaft as the centre of the circle, and the approximate average linear speed of the reel was calculated by multiplying the radius of the minimum inscribed circle of the relative motion trajectory of the reel by the crank angular velocity. The speed ratio for the new tine bar was then calculated using [eq. (24)]:

$$\begin{cases} \lambda = \frac{\omega R}{v_m} \\ \omega = \frac{\pi n}{30} \end{cases} \quad (24)$$

Where:

$\lambda$  is the speed ratio of the tine bar;

$\omega$  is the angular speed of the reel ( $\text{rad}\cdot\text{s}^{-1}$ ),

$R$  is the radius of the minimum inscribed circle of the relative motion trajectory of the tine bar (m);

$v_m$  is the forward speed of the windrower ( $\text{m}\cdot\text{s}^{-1}$ ), and

$n$  is the speed of the reel transmission shaft ( $\text{r}\cdot\text{min}^{-1}$ ).

Fig. 10 shows the relative and absolute motion trajectories formed by the new reel for a reel speed ratio of 1.8 and a forward speed of  $1 \text{ m}\cdot\text{s}^{-1}$ . From the figure, it can be seen that the planar five-link mechanism forms a larger ring buckle when the speed ratio is as described above, which enhances its ability to handle tall rapeseed plants. In addition, the relative motion trajectory of the new reel is not circular; after pushing the rapeseed onto the header, the curve radius and curvature of its motion trajectory are significantly reduced, and this curve is basically close to a straight line. Hence, at this trajectory, the tine bar will quickly shrink away from the rapeseed plants, meaning that the tine bar can quickly retract after completing the push of the rapeseed plants. The movement characteristics of the tine bar are very beneficial in terms of preventing rapeseed plants from being entangled on the reel or picked out from the header, thereby improving the quality of operation and reducing the losses caused by the rapeseed windrower.

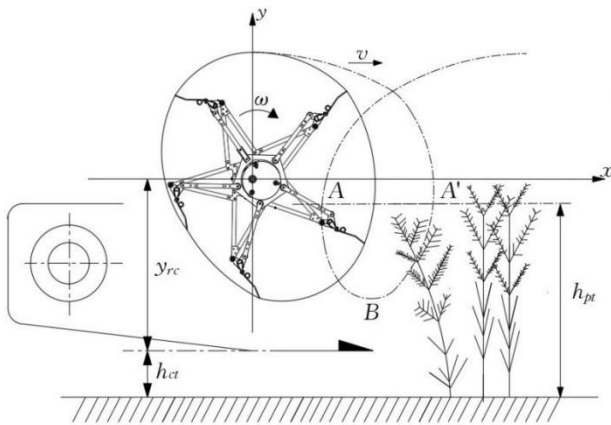


FIGURE 10. Relative position of the reel on the header of the windrower ( $v$  is the machine forward speed (m/s);  $y_r$  is the distance from the reel shaft to the ground (m);  $h_{ct}$  is the plant cutting height (m);  $y_{rc}$  is the vertical distance between the reel axis and the cutting bar plane (m);  $h_{pt}$  is the distance from the horizontal AA' line to the ground, which is consistent with the average height of rapeseed plants (m); AA' is the longest transverse chord of the buckle (m); and B is the point where the speed is horizontally backward).

The position of the reel relative to the front and rear of the header, and the height of the reel relative to the header, directly affect the quality and efficiency of reel operation. It is therefore necessary to set the installation parameters of the reel on the header correctly. Firstly, to enable the reel to guide the rapeseed to be cut, support the rapeseed plants during cutting, and push the cut rapeseed plants backwards, the reel must have a horizontal backward speed relative to the forward

direction of the machine after contact with the rapeseed. Over the entire buckle trajectory (as shown in Fig. 10), only the portion of the trajectory below the longest transverse chord AA' of the buckle has a horizontal backward speed. The speed of the tine bar at point A is vertically downward, the speed at point A' is vertically upward, and the speed at point B is horizontally backward, meaning that the tine bar only has the function of backward plucking within the trajectory range ABA' of the string. In order to improve the quality of harvesting and reduce the damage caused by the reel hitting the rapeseed, it is necessary to adjust the reel so that the cutter is directly below point B. When determining the position of the reel in the vertical direction, the distance between the reel shaft and the ground must meet the condition in [eq. (25)]. In addition, it is also necessary to adjust the specific horizontal position of the reel according to the height and other parameters of the rapeseed plants in real time, to achieve ideal reel operation. In the analysis of the reel kinematics, the plant cutting height ( $h_{ct}$ ) is considered to be known.

$$\begin{cases} y_r = h_{ct} + y_{rc} \\ y_r \leq h_{pt} + \frac{R}{\lambda} \end{cases} \quad (25)$$

Where:

$y_r$  is the distance from the reel shaft to the ground (m);

$h_{ct}$  is the plant cutting height (m);

$y_{rc}$  is the vertical distance between the reel axis and the cutting bar plane (m), and

$h_{pt}$  is the distance from the horizontal AA' line to the ground, which is consistent with the average height of the rapeseed plants (m).

According to [eq. (25)], the vertical position of the reel axis above the cutting bar plane can be calculated using [eq. (26)]. In addition, for efficient action of the reel, to avoid excessive bending of the plants, and to reduce the disturbance caused by the reel to the rapeseed plants, the vertical position of the reel axis above the cutting bar plane should not only meet [eq. (26)], but the bar of the reel should also act at or above the centre of gravity of the rapeseed plant. The centre of gravity of a rapeseed plant is generally located at about one-third of the length from the top of the cut part.

$$y_{rc} \leq h_{pt} - h_{ct} + \frac{R}{\lambda} \quad (26)$$

## Experimental materials and equipment

The experiment was conducted on 8<sup>th</sup> September 2022, in a rapeseed field in Zhangye City, Gansu Province. Rapeseed plants with neat growth and no lodging in the entire field were selected, and the experiment was started when about 80% of the pods began to turn yellow. The variety of rapeseed was Ganyouza No. 1, which was planted through mechanical direct seeding. The planting density was 3.5 plants per square metre, with an average plant height of 1.6 m, a bottom pod height of 0.8 m and a fruit pod canopy diameter of 0.6 m. In addition, during the cutting and sunning

experiment, the moisture content of the rapeseed stems was 76.5% and the weight of 1,000 seeds was 3.5 g. The equipment used in the experiment included the original cutting and sunning header and the new one. Except for the differences in the structure of the newly designed reel and cutting mechanism compared to the original one, all the other mechanical parts had the same structure, and all of the operating parameters of the two cutting and sunning headers remained consistent throughout the experiment.

### Experimental method

In order to verify the differences in the two core work indicators of laying quality and loss rate for the newly designed and existing rapeseed headers of the windrower, cutting and sunning experiments were conducted. The ratio of the conveyor belt speed to the machine forward speed was 1.8; the ratio of the tine bar speed of the reel to the forward speed of the machine was 1.8; and the ratio of the cutter speed to the machine forward speed was 1.2. The height of the header from the ground was kept at 0.3 m. During the experiment, the forward speeds of the machine were 0.6, 0.8, 1, 1.2, and 1.4 m.s<sup>-1</sup>, respectively. The experiment was repeated three times at each operating speed, and the average value was calculated as the final result.

### Test of laying quality

The laying quality indicators for rapeseed plants were calculated for the two different windrowers according to the methods specified in the relevant Chinese standards (GB/T8097-2008). According to these national standards, the length of each test area was set to 25 m. In each experiment, 25 measuring points were selected in the measuring area, spaced 1 m apart. The laying width  $l_i$  at each measuring point was measured with a tape measure, and the laying height  $h_i$  was measured with a steel tape measure. One rapeseed plant from each of the upper and lower layers was selected at each of the measuring points, and the upper layer laying angle  $\theta_{iup}$  and lower layer laying angle  $\theta_{idown}$  were measured with an angle ruler. The laying angle for each rapeseed plant was calculated using [eq. (27)].

$$\theta = \frac{1}{25} \sum_{i=1}^{25} \left( \frac{\theta_{iup} + \theta_{idown}}{2} \right) \quad (27)$$

Where:

$\theta$  is the laying angle (°).

The difference in laying angle between the upper and lower layers was calculated using [eq. (28)]:

$$\Delta\theta = \frac{1}{25} \sum_{i=1}^{25} \left| \bar{\theta}_{iup} - \bar{\theta}_{idown} \right| \quad (28)$$

Where:

$\Delta\theta$  is the difference in laying angle between the upper and lower layers (°);

$\bar{\theta}_{iup}$  is the average laying angle of the upper stem (°), and

$\bar{\theta}_{idown}$  is the average laying angle of the lower stem (°).

The consistency of the laying width was evaluated by calculating the variation coefficient for the laying width under several combinations of working parameters. The variation coefficient was calculated using [eq. (29)]:

$$CV_l = \frac{\sqrt{\frac{1}{25} \sum_{i=1}^{25} (l_i - \bar{l})^2}}{\bar{l}} \times 100\% \quad (29)$$

Where:

$CV_l$  is the coefficient of variation of laying width (%), and  $\bar{l}$  is the average laying width (m).

The coefficient of variation in the laying height for each combination of parameters was calculated by [eq. (30)] to evaluate the consistency of the laying height:

$$CV_h = \frac{\sqrt{\frac{1}{25} \sum_{i=1}^{25} (h_i - \bar{h})^2}}{\bar{h}} \times 100\% \quad (30)$$

Where:

$CV_h$  is the coefficient of variation for the laying height (%), and

$\bar{h}$  is the average laying width (m).

### Experimental study of the impact of different windrowers on the final harvest loss rate

In order to compare the differences in the impact of two types of windrowers on the total loss rate of rapeseed harvest, the loss rates after picking and threshing using different windrower headers were measured in the field. First, the rapeseed in each different experimental area for the different windrowers under different motion parameters was labelled. Then, when the rapeseed had been harvested and dried for five days and met the threshing conditions, a combine harvester equipped with a rapeseed picking table was used for picking and threshing operations. Before the picking and threshing operation, the yield for each group of experiments using different windrowers and machine motion parameters was measured. The quality of the rapeseed left in the field for different experimental groups was then measured after picking and threshing. Finally, the total loss rate of rapeseed harvest in each group of experiments was calculated with [eq. (31)], and this indicator was used to evaluate the impact of the different windrower headers on the total loss rate of rapeseed harvest under different operating parameters.

$$S_t = \frac{w_t}{\sum W} \times 100\% \quad (31)$$

Where:

$S_t$  is the total loss rate of rapeseed (%);

$w_t$  is the total mass loss of rapeseed in each experimental group (g), and

$\sum W$  is the rapeseed grain yield for the corresponding experimental group (g).

## RESULTS AND DISCUSSION

### Laying quality for different windrower headers

The test results for the laying quality of the windrowers are shown in Table 1, and it can be seen that the structure of the reel has an impact on the work quality of the windrowers. There are significant differences between the operational quality indicators for the new header and the old one. The average laying angle of the rapeseed stalks harvested by the new header is no more than 30°, and the average difference in laying angle is only 42.9% of the corresponding value for the original header. The coefficients of variation for

the laying height and laying width are also smaller than the corresponding values of the original header. In addition, the reel of the new header did not entangle or throw out rapeseed plants during the experiment. The heads of the rapeseed plants harvested with the new header did not land on the ground, which is conducive to proper drying and reducing the loss rates of later picking and harvesting. The forward speed of the windrower had a significant impact on the quality of the original header; as the speed of the machine increased, the entanglement of the rapeseed plants in the old reel became increasingly serious, and the number of cut rapeseed plants thrown out of the header by the reel also increased.

TABLE 1. Results of laying quality tests.

Forward speed of the windrower (m.s <sup>-1</sup> )	Laying angle (°)		Difference in laying angle between upper and lower layers (°)		Coefficient of variation in laying height (%)		Coefficient variation in laying width (%)	
	New header	Original header	New header	Original header	New header	Original header	New header	Original header
0.6	25.3	31.7	5.1	13.4	6.4	7.9	7.6	9.2
0.8	26.6	35.4	5.7	13.1	6.8	7.8	8.4	9.4
1	27.3	37.5	6.2	13.6	7.5	9.2	8.4	8.6
1.2	28.2	39.8	6.5	15.8	8.6	8.7	9.2	9.8
1.4	28.5	42.6	7.3	15.2	8.2	9.4	9.3	10.1
Mean value	27.2	37.4	6.1	14.2	7.5	8.6	8.6	9.4
Standard deviation	1.3	4.2	0.8	1.2	0.9	0.7	0.7	0.6

To investigate the significant differences in the impact of the different headers and different operating parameters on the quality of operation, a two-way analysis of variance was conducted on the experimental data for the laying quality. A normality test (based on Shapiro Wilk method) and a homogeneity test of variance (Levene's test method) were first applied to the total loss rate data corresponding to different headers under different operating parameters, and the results showed that the experimental data had a normal distribution and homogeneity of variance. A two-way analysis of variance was then performed on the experimental data. The results for the laying angle indicator indicated that the P value for the speed was 0.125, while the P value for the type of the header was 0.001; hence, at the 0.05 level, the operating speed of the windrower had no significant impact on the laying angle, whereas the type of windrower had a significant impact. The results of the two-way analysis of variance for the difference in laying angle between the upper and lower layers indicated that the P value for the speed was 0.058, while the P value for the type of windrower header was 0.00002. Hence, at the 0.05 level, the forward speed of the windrower had no significant impact on the difference in laying angle between the upper and lower layers, whereas the header type of windrower had a significant impact. The results of the two-way analysis of variance for the coefficient of variation index of the laying height indicated that the P value for the speed was 0.053, and the P value for the type of windrower was 0.017, meaning that at the 0.05 level, the forward speed of the windrower had no significant impact on the coefficient of variation of the laying height, whereas the type of windrower had a significant impact on this indicator. The results of a bivariate analysis of variance for the coefficient of variation

index of laying width indicated that the P value for the forward speed was 0.072, while the P value of the type of windrower was 0.022; thus, at the 0.05 level, the forward speed of the windrower had no significant impact on the coefficient of variation of rapeseed laying width, whereas the type of windrower had a significant impact. From these results, it can be seen that the new header for the windrower can significantly improve the quality of operation, while the work speed has no significant impact on its performance.

### Experimental results for the impact of different headers on the total harvest loss rate

The experimental results for the total harvest loss rate for the different headers at different forward speeds are shown in Fig. 11. For the same forward speed of the machine, the total loss rate for the new header was relatively small. Within the machine's forward speed range of 0.6–1.4 m.s<sup>-1</sup>, the average total loss rate for the new header was 16.4% lower than for the original header, although the total loss rates for both headers increased with the machine's forward speed. When the forward speed of the machine was increased from 1 m.s<sup>-1</sup> to 1.4 m.s<sup>-1</sup>, the loss rate for both headers rapidly increased. The main reason for this is that with an increase in the forward speed, the speed of the cutting knife and reel also increase, which increases the disturbance from these mechanisms on the brushing and hitting of rapeseed plants, leading to more rapeseed pods rupturing or falling off. In order to explore the significance of the impact of the different headers and forward speed of the machine on the total loss rate, a two-way analysis of variance was conducted on the experimental results. A normality test (using the Shapiro Wilk method) and a homogeneity test of variance (by the Levene's test method) were first applied to the experimental data, and

the results showed that the experimental data met the conditions for a normal distribution and the homogeneity of variance. A two-way analysis of variance was then performed on the experimental data. The results indicated that the P value for the machine's forward speed was 0.027, and the P value for the header type was 0.003, meaning that both the forward speed of the machine and the type of the header both had a significant impact on the loss rate.

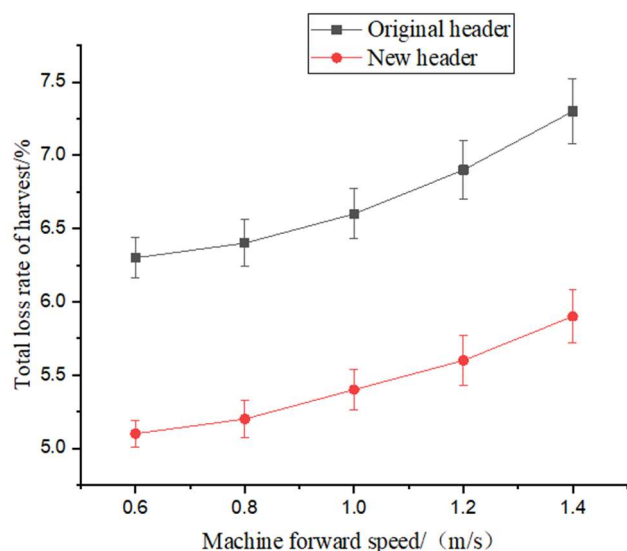


FIGURE 11. Experimental results for the impact of different headers on the total harvest loss rate.

### Key technologies of the new rapeseed header

In response to a series of problems such as poor quality and high loss rates in the cutting and sunning operations of tall, thick stems of rapeseed planted in China, a new type of rapeseed header for a windrower was designed in this study to improve the cutting and drying quality of rapeseed and to reduce the loss rate caused by the operation of the windrower. The main factors affecting the quality of rapeseed plant placement and the loss rate caused by windrower are the reel and the cutting mechanism (Wan et al., 2018). This study has therefore presented an innovative design for the reel and cutting system based on the original header of the windrower. Firstly, a five-link mechanism with a planar double-crank driven reel was designed, the key parameters were determined and a theoretical analysis of the new reel was carried out. The results of an analysis of the motion of the new reel showed that compared to the ordinary reel (Jiang et al., 2022), its motion trajectory is particularly suited to tall, thick rapeseed stems; its operational ability is strong, and it is not easy to cause entanglement of rapeseed plants on the reel. These characteristics of the new reel have a positive effect on improving the quality of operation of the windrower. A double-action cutter driven by a planetary gear mechanism was then designed. A theoretical analysis of the new cutting mechanism showed that it not only has characteristics such as high cutting continuity, stable load, and small disturbance to rapeseed stems, but also has advantages such as a low motion inertia force and low power consumption compared to a single moving blade driven by the widely used linkage mechanisms or swing ring mechanisms in a windrower. These characteristics of the new cutting mechanism make it very advantageous for cutting tall, thick rapeseed stalks.

### Operational performance of the new header of windrower

Our experimental results showed that the overall performance of the new header was superior to the original one, a finding that is consistent with the results of the theoretical analysis. Firstly, the indicators of laying quality for the windrower equipped with the new header were better than for the original one; the reel of the new header did not entangle or throw out rapeseed plants during the experiment, indicating that its special reel trajectory does indeed give it good operational performance. Furthermore, the impact of the forward speed of the windrower on the laying quality was not significant for either the new or the existing header, whereas the machine forward speed and type of header did have a significant impact on the rapeseed loss rate. These conclusions are consistent with those of other scholars (Dodds et al., 1967a). More importantly, the average total loss rate of rapeseed caused by the new header was 16.4% lower than for the original header, indicating that the new header was beneficial in terms of reducing the loss rate of rapeseed during harvest. As the speed of the windrower increased, the loss rate increased for both types of windrower. The main reason for this is that with an increase in the machine's forward speed, the speeds of the cutting knife and reel also increase, which increases the disturbance caused by these mechanisms in terms of the brushing and hitting of rapeseed plants, leading to more rupture or detachment of rapeseed pods. These results are also consistent with the conclusions of other scholars (Dodds et al., 1967b).

### Limitations of this study and potential future work

Although the theoretical analysis carried out in this study showed that the new cutting mechanism had an advantage in terms of reduced power, the significance of the actual difference in power consumption between the new cutting mechanism and existing similar cutting mechanisms was not explored. In future work, power consumption testing could be conducted on the new cutting mechanism to quantitatively study its actual performance in regard to energy conservation. Through the use of high-speed cameras or other means, the disturbance effects of the new cutter on rapeseed stems during actual operation could be observed, and its performance in reducing the harvest loss rate of rapeseed could be analysed. In addition, applying this new type of reel and cutting mechanism to harvesting machinery for crops such as sesame, which are prone to significant losses during harvesting, will also be of great importance to improve the operational performance of the harvester.

### CONCLUSIONS

In order to solve a variety of problems associated with cutting and drying operations of tall, thick rapeseed plants with the original rapeseed windrower, this study has presented a new type of header for these operations. The reel of the new header is driven by a five-link mechanism with planar double cranks, while the horizontal cutter system is a double-action cutter driven by a planetary gear mechanism. The results of both a theoretical analysis and experiments indicated that compared to the original header, the new one can significantly improve the quality of operation for tall, thick rapeseed plants, and can reduce the rapeseed loss rate caused by the windrower.

## ACKNOWLEDGMENTS

This work was supported by the Scientific and Technological Planning Projects of First Division Alar City, Xinjiang Construction Corps (Grant No. 2022ZB04).

## REFERENCES

- Chai XY, Xu LZ, Yan C, Liang ZW, Ma Z, Li YM (2018) Design and test of cutting frequency follow-up adjusting device for vertical cutting knife of rapeseed cutting machine. *Trans CASM* 49: 100–106.
- Dodds ME (1967a) A review of research on the use of the windrower for harvesting cereal crops. *Canadian Agricultural Engineering* 9: 23-26.
- Dodds ME (1967b) Observations of the performance of a self propelled windrower. *Canadian Agricultural Engineering* 2: 70–75.
- Guan ZH, Jiang T, Li HT, Wu CY, Zhang M, Wang G, Mu SL (2021) Analysis and test of the laying quality of inclined transportation rape windrower. *Transactions of the Chinese Society of Agricultural Engineering (Transactions of the CSAE)* 37(4): 59-68.
- Guan ZH, Wu CY, Wang G, Li HT, Mu SL (2019) Design of bidirectional electric driven side vertical cutter for rape combine harvester. *Transactions of the Chinese Society of Agricultural Engineering he CSAE)* 35(3): 1-8.
- Jiang T, Zhang M, Guan ZH, Mu SL, Wu CY, Wang G, Li HT (2022) Simulation and analysis of the pneumatic recovery for side-cutting loss of combine harvesters with CFD-DEM coupling approach. *International Journal of Agricultural & Biological Engineering* 15(2):117–126.
- Li Y, Xu LZ, Gao ZP, Lu E, Li YM (2021) Effect of vibration on rapeseed header loss and optimization of header farne. *Transactions of the ASABE* 64: 1247–1258.
- Liang SN, Mu SL, Tang Q, Zhang M, Wu CY (2018) The effect of different harvest methods on formation of rape harvest loss. *Journal of Agricultural Mechanization Research* 40(3): 134-140.
- Ma LN, Wei JY, Huang XM, Zong WY, Zhan GC (2020) Analysis of harvesting losses of rapeseed caused by vibration of combine harvester header during field operation. *Transactions of the Chinese Society of Agricultural Engineering* 51:141–145.
- Qing YR, Li YM, Xu LZ, Ma Z (2021) Screen oilseed rape (*Brassica napus*) suitable for low-loss mechanized harvesting. *Agriculture* 11:504.
- Ran JH, Mu SL, Li HT, Guan ZH, Tang Q, Wu CY (2020) Design and test of planet gear driver of reciprocating double-acting cutter for rapeseed combine harvester. *Transactions of the Chinese Society of Agricultural Engineering* 36:17–25.
- Ren SG, Jiao F, Wu ML, He SZ, Tang SZ (2018) Studies of united harvest machine cutting system structure parameters on the vibration impact. *Journal of Agricultural Mechanization Research* 40(11): 38-43.
- Shen C, Li XW, Zhang B, Tian KP, Huang JC, Chen QM (2016) Bench experiment and analysis on ramie stalk cutting. *Transactions of the Chinese Society of Agricultural Engineering* 32(1):68-76.
- Sun Y, He ZY, Xu JQ, Sun W, Lin GB (2023) Dynamic analysis and vibration control for a maglev vehicle-guideway coupling system with experimental verification. *Mechanical Systems and Signal Processing* 188: 109954.
- Wan XY, Liao QX, Yang X, Yuan JC, Li HT (2018) Design and evaluation of cyclone separation cleaning devices using a conical sieve for rape combine harvesters. *Applied Engineering in Agriculture* 34(4):677–686.
- Wang G, Guan ZH, Mu SL, Tang Q, Wu CY (2017) Optimization of operating parameter and structure for seed thresher device for rape combine harvester. *Transactions of the Chinese Society of Agricultural Engineering* 33: 52–57.
- Wu CY, Wang JJ, Liao QX, Wang ZH, Wu WK (2017) Current status and problems of rapeseed production. *Journal of Chinese Agricultural Mechanization* 38(1): 124-131.
- Wu WJ, Wu CY (2018) Research status of header of rapeseed combine harvester. *Jiangsu Agricultural Sciences* 46(7): 5-11.
- Yang HM, San YL, Chen YF, Wang XN, Niu CH, Hou SL (2019) Influence of different vibration characteristic parameters on vibration response of apricot trees. *Transactions of the Chinese Society of Agricultural Engineering* 35:10–16.
- Zhan G, Ma L, Zong, W, Liu W, Deng D, Lian G (2022) Study on the vibration characteristics of rape plants based on high-speed photography and image recognition. *Agriculture* 12: 727.